LA-UR-18-21549
Approved for public release; distribution is unlimited.

Title: Probability of Encounter Between Ports of Entry (PrEP): Aversion Force-Field “Early Validation” Report

Author(s): Ambrosiano, John Joseph
Dauelsberg, Lori Rose
Tompkins, George

Intended for: Report

Issued: 2018-02-27

Probability of Encounter Between Ports of Entry (PrEP): Aversion Force-Field "Early Validation" Report

John Ambrosiano, Lori Dauelsberg, George Tompkins

February 27, 2018

Overview

To enhance detection and interdiction of radiological or nuclear material trafficking between primary POEs into the US, The Department of Homeland Security is faced with highly variable smuggling pathways through expansive geographic regions. The goal of this project is to test an approach to estimating likely pathways, as well as the probability of encounter along any given route.

Our goal is to test the feasibility of a novel approach based on assessing the adversary's perception of discovery likelihood over a broad geographic region, and using that result to estimate an "aversion force field" over the same region. The aversion force field is derived from analogies based on the physics of electric charges. Combining the aversion force with the intention of an adversary to reach their destination, generates a route that is consistent with both the adversary's intention and their aversion to deterrent measures.

Phase I is exploratory. Its goal to demonstrate the feasibility of the approach. This report describes progress in an essential part of the approach, specifically, to implement and couple two principle model components: (1) the Bayesian network model of an adversary's perception of discovery likelihood; and (2) the physics-inspired aversion field model. The objective is to show that the field produced from the two components is plausible and consistent with the assumptions and the data.

Figure 1 illustrates the workflow of this phase to the present stage. After collecting preliminary data and implementing each of the two model components, they were separately evaluated. Following this step, the output from the Bayesian network was input to the aversion field solver, and the combined results evaluated as reported here.

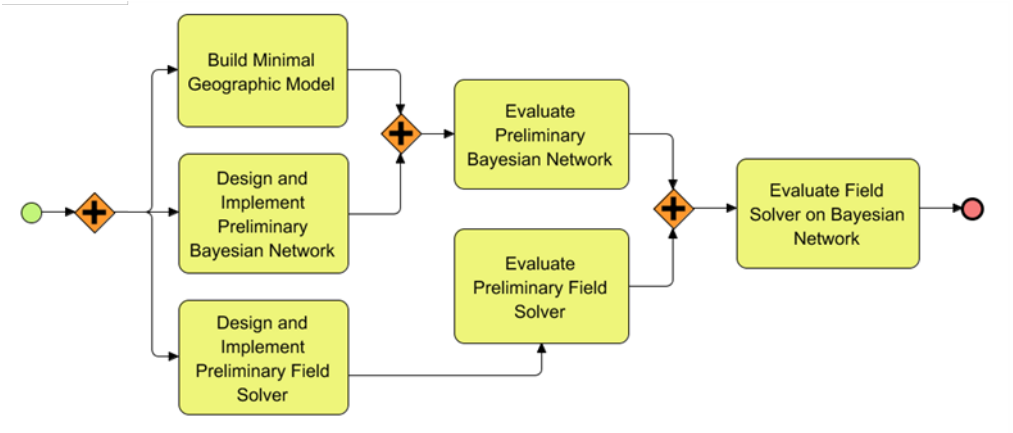

Figure 1. The development workflow for demonstrating plausibility of the aversion field solution.

Design, Implementation, and Evaluation of the Bayesian Network Model

The initial Bayesian network assumes infiltration on foot by an adversary whose aim is to reach their destination without being observed. It is based on U.S. Army Field Manual FM 7-93.[1] The doctrine described in the manual holds that infiltrators will prefer surroundings that make them hard to observe and unlikely to encounter.

Based on this principle, a preliminary Bayesian model was developed that requires no initial subject matter input, relying only on geographic terrain and population features. A network diagram of the model is shown in Figure 2. We assumed a uniform, low-level population density for the sparsely-populated test region. The other input grids used for the initial test are shown in Figure 3.

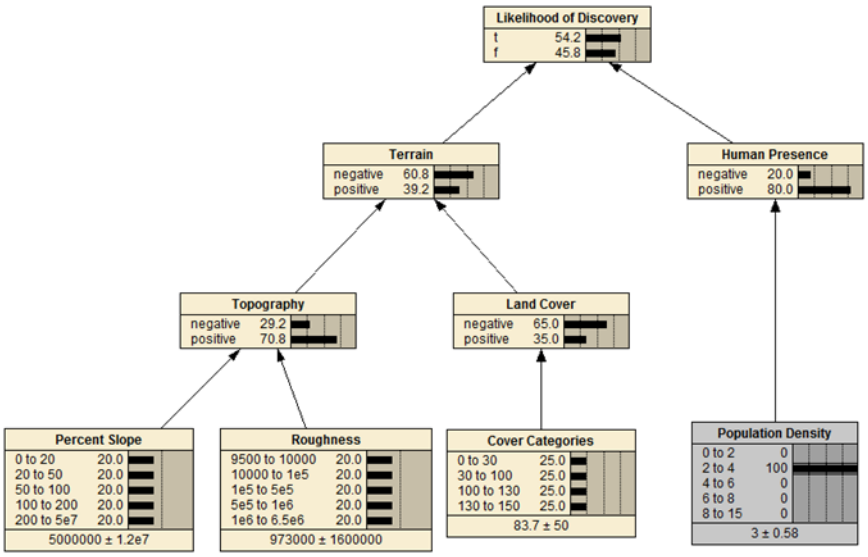

Figure 2. The preliminary Bayesian network model based on US Army Field Manual 7-93.

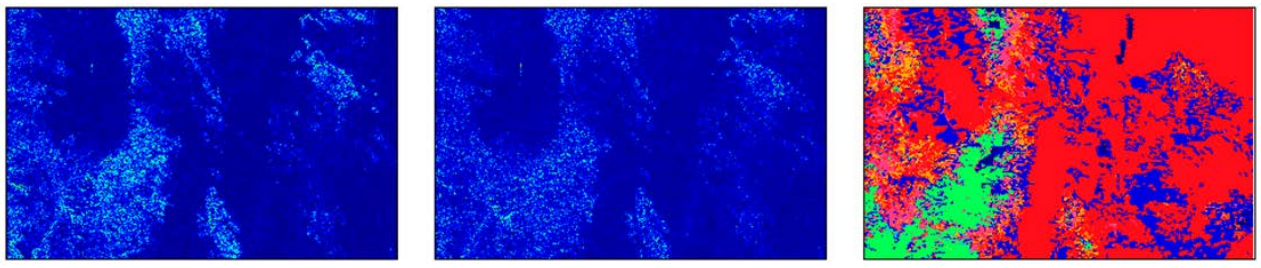

Figure 3. The input grids for the Bayesian network. From left to right: percent slope, roughness, and land cover category.

The output of the Bayesian network based on these inputs is shown in Figure 4. From the legend, one can see that the results largely partition the test region in to moderately low (~30%) and moderately

[1] United States Army Field Manual 7-93 Long-Range Surveillance Unit Operations.

high (~70%) discovery probabilities. This is likely the result of strong correlations over broad regions between the two factors derived from terrain elevation (percent slope and roughness), and ground cover type.

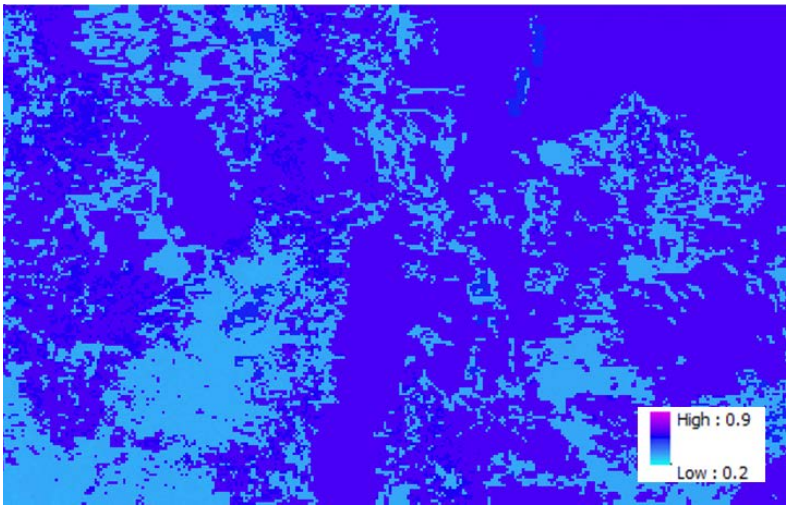

Figure 4. The output of the Bayesian network model (probability of discovery) over the geographic test region.

Design, Implementation, and Evaluation of the Aversive Force Field Model

The aversion force field model is based on an analogy between the presence of deterrent features in a geographic landscape, and repulsive electric fields resulting from the spatial distribution of electric charges. In electrostatics, a complex distribution of charge over space can be represented by a charge density field which is the source of an electric potential energy landscape. The direction and magnitude of the electric force at any point in the potential field is proportional to the negative gradient of the potential at that point. In other words, a charge placed in the potential field will seek a lower potential energy in the direction of steepest descent, the way a ball placed on a hill will roll downward.

The differential equation that defines the electric potential in terms of the charge source density is Poisson's Equation:

$$\nabla^2 \emptyset = -k\rho \qquad (1)$$

where $\emptyset$ is the potential field, ∇^2 is the differential Laplacian operator, and ρ is the charge density field. The constant *k* is an arbitrary, positive scale factor that determines the relative strength of the potential field given the magnitude of the charge density. For our purposes, we set *k=1* without loss of generality.

Given the potential $\emptyset$ from Poisson's equation, the force at a specific location $\vec{x}$ is given by $\vec{F} = -q\nabla\emptyset$

where *q* is the pseudo-charge assigned to an adversary agent of a given type.

Equation 1 must be converted to a discrete form to solve numerically on a grid. The usual method is to substitute finite differences for differentials in the Laplacian operator. Using a symmetric finite difference stencil in two dimensions the difference form of Poisson equation becomes:

$$\nabla^2 \emptyset = -k\rho \rightarrow \frac{\emptyset_{i+1,j} - 2\emptyset_{i,j} + \emptyset_{i-1,j}}{\delta x_{i,j}^2} + \frac{\emptyset_{i,j+1} - 2\emptyset_{i,j} + \emptyset_{i,j-1}}{\delta y_{i,j}^2} = -k\rho_{i,j} \qquad (2)$$

The *(i,j)* indices in Equation 2 label the centers of the cells of the grid, while $\delta x_{i,j}$ and $\delta y_{i,j}$ are the approximate local dimensions of cell *(i,j)* in the x and y directions respectively. The local cell widths are approximate, even on a regular geographic grid, as a result of geodesics.

The difference expressions of Equation 2 are applied to each cell of the grid forming a sparse $(M \times N)^2$ matrix, where *M* and *N* are the number of cells in the *x* and *y* directions respectively. Because the number of equations grows as the square of the number of cells, the computational resources required to solve the equation grows quickly with the grid size.

The matrix equation to be solved is

$$DU = -R \qquad (3)$$

where *D* is the matrix of differences, *U* is the matrix of potential field values, and *R* is the matrix of source values. Boundary conditions representing values, either of Ø or its normal derivative, are required. In the discrete formulation, this translates to either a set of given values for *U,* or a set of given differences adjacent to the left, right, top, and bottom cells of the grid. These conditions are embedded in the finite difference matrix *D*.

There are a number of ways to solve Equation 3. We have used two different approaches. The most straightforward is the "direct" method. This method attempts to find the inverse of *D* directly. The method is costly for equations involving large sparse matrices. Our attempts to use this method began to fail when the matrix became larger than approximately *300 x 300* cells. Iterative methods are another class of solvers. At the time of this report, iteratives methods appeared to be more successful for solutions on large grids.

We require large grids to ameliorate the influence of fixed boundary conditions when charge sources are near the boundaries, as boundary conditions in that case dominate the solution for the potential in the interior. In our application, we expect to have substantial source values everywhere in the region of interest.

We have found that adding rows and columns of empty buffer cells, whose extent is approximately equal to that of the grid in each dimension, are necessary to avoid such effects when charges are near the edge of the solution region. This finding is consistent with the application of such methods to electrostatic boundary problems appearing in the literature.

The need for large buffer zones results in grids that are nearly an order of magnitude larger than the problem region. This in turn implies a matrix sizes nearly two orders larger than the number of cells required for grid covering the region of interest alone. Such rapidly unfavorable scaling drives the requirement for employing the most computationally efficient methods to solve for the potential in the aversion force model.

A simple test of the field solution is shown in Figure 5. On the right, the line charge shown in red generates the potential field on the left. The force arrows superimposed on the right are derived from the potential. One can easily see that large forces directed away from the line charge appear near the source and diminish with distance. Sampling the potential shows it is consistent with to the $1/r$ force potential law for electrostatics. In application, the line charge would represent an extended deterrent

feature such as border fence. An adversary would feel the force very strongly near the fence, but the effect would diminish quickly with distance.

Integrated Bayesian Network and Aversion Force Calculation

To generate an aversion force field, we input the probability field of Figure 4 as the source in the matrix equation (Equation 3). For test purposes, we first coarsened the source grid to produce the grid pictured in Figure 6.

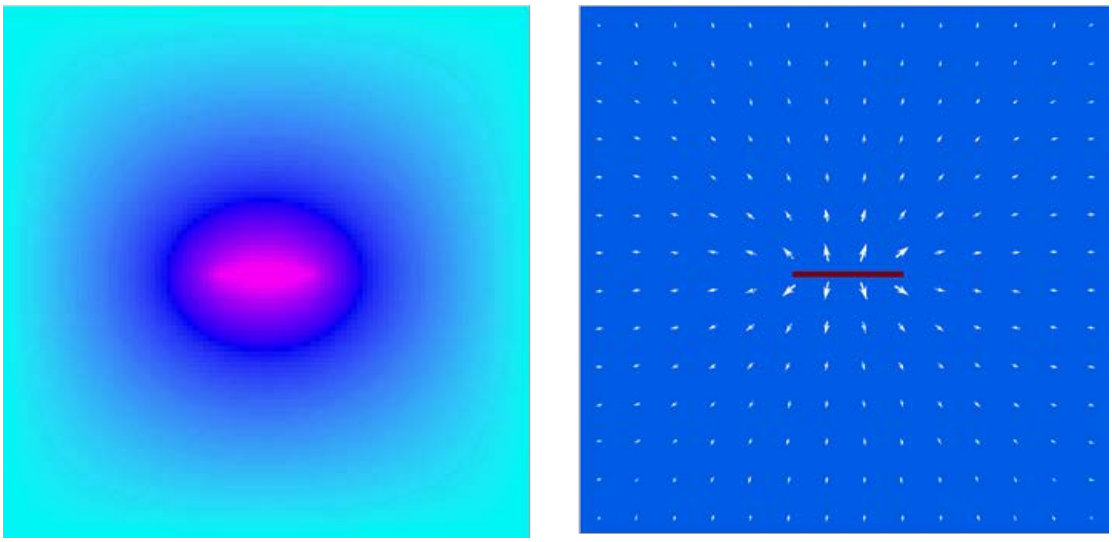

Figure 5. A simple test of the force calculation. On the right, the charge in red generates the potential field at the left. The force arrows on the right are derived from the potential.

The potential and force fields are shown superimposed in Figure 7. One can see from the figure that the force field is most intense near the maxima of the potential field as expected. Figure 8 shows the force field superimposed on the source field. Here it is clear that an adversary that finds themselves in a region where the discovery probability is high would feel a strongly aversive force directed from their present position to one where the probability of discovery is much lower.

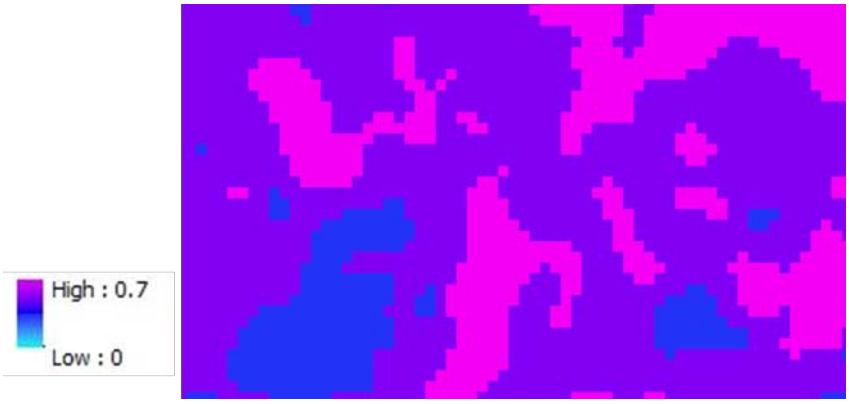

Figure 6. A coarsened grid of source values for the field solution test.

Agent Movement Test

The next step in the project is to develop the agent model, the last of the critical model components, and integrate it with the Bayesian network and force-field models to demonstrate feasibility of the overall approach.

Although not prepared to fully develop and integrate the agent model at this stage, it is worthwhile to implement a portion of the agent model to show that aversion fields derived from a discovery likelihood source produce plausible agent movement. For this purpose we have implemented an agent "mover". This is a sub-model that computes the force at an agent's location and moves it one step, that is, updates the agent's position and velocity.

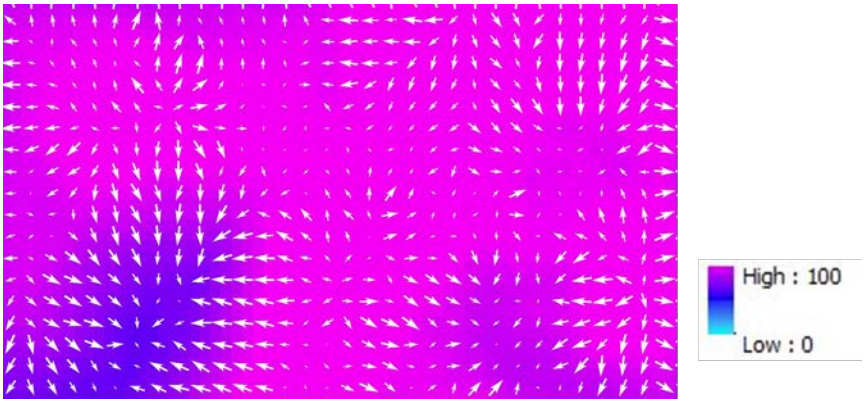

Figure 7. The potential field derived from the source grid with force vectors superimposed.

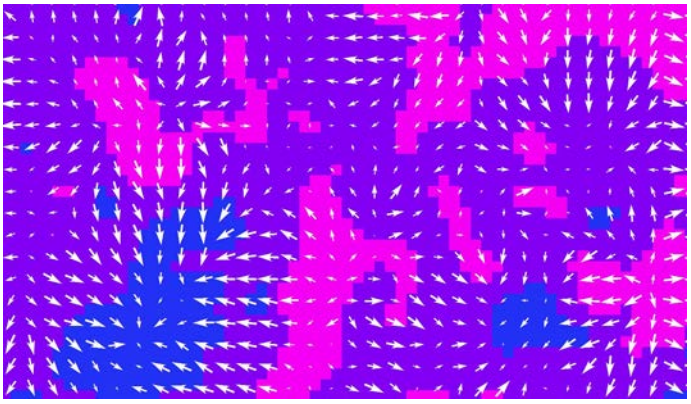

Figure 8. Force-field vectors superimposed on the source field.

The force on an agent at any point in the landscape is the sum of two forces: (1) the "intention" force, and (2) the aversion force. The computation of the aversion force we have just described and demonstrated. The intention force is the force that would attempt to restore the intended direction and speed of movement of an agent if their current velocity were different. The complete influence of these forces on agent motion is governed by Equations (4-7).

$$\vec{a}_a(x,t) = f_\delta \vec{A}_a(x(t)) \qquad (4)$$

$$\vec{a}_i(t) = \frac{(\overrightarrow{v_0}(t) - \vec{v}(t))}{\tau} \quad (5)$$

$$\vec{a}(x,t) = \vec{a}_i(x,t) + \vec{a}_a\,(x,t) \quad (6)$$

$$\vec{v}(t+\delta t) = \vec{v}(t) + \vec{a}(x,t)\delta t \quad (7)$$

The acceleration due to aversion is given by Equation 4, where $f_\delta \vec{A}_a$ is analogous to $\frac{q}{m}\vec{E}$ in physics where $\vec{E}$ is the electric field vector. In physics, the charge-to-mass ratio *q/m* describes the ability of an electric field of a given strength to deflect a charged particle from its current direction. Increasing the charge *q* increases the acceleration for a given field strength, whereas increasing the mass *m* raises the particle's inertia making it harder to deflect. In our application, $\vec{A}_a$ is analogous to the electric field. We replace *q/m* with f_δ which we call the deflection factor.

In Equation 5, the acceleration due to the agent's desire to recover its goal direction and intended speed is defined in terms of the difference between its current velocity $\vec{v}$ and its intended direction and speed $\overrightarrow{v_0}$ divided by an arbitrary reaction time τ.

Equation 6 is the total acceleration which, when applied in Equation 7, updates the agent's velocity, which in turn leads to a displacement of the agent within the same time interval.

Implementing these equations in a prototype agent mover, we have generated ten paths by starting agents at locations spaced along the southern boundary of Figure 8, with the destination of each agent being a point centered on the top boundary. For this test, we have set the deflection factor to 2, and the reaction time to one time step. The intended speed is 5 km/hour, and the time step is 15 minutes.

The results are shown in Figure 9. Here we have changed the color palette from that in Figure 7 to make subtle differences in the potential field easier to see. We have also added an internal border for purposes of illustration.

We see that the contours of the aversion potential lead agents introduced near the minimum potential on the left (west) to move toward the low potential region there, and then to funnel along that portion of the landscape toward their common destination.

On the right (east), where the potential appears high to the agent's left, agents introduced on that side prefer to move right where the potential appears relatively lower. As they attempt to move northwest toward their common destination, they encounter very high aversion potentials and are therefore forced to move northeast.

These movements are consistent with the assumptions of the model and are considered to be very plausible. Were these results based on a carefully calibrated model and input data, they would suggest that, at narrow portions of the western border, and at somewhat broader segments of the eastern border, interdiction might be favorable.

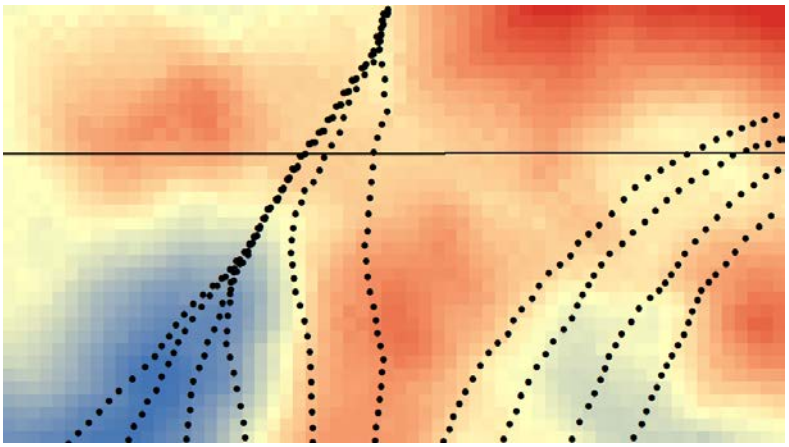

Figure 9. The aversion potential field with the trails produced by ten agents moving across the aversion field towards a common destination centered on the top boundary.

Summary

In this report, we described an initial implementation of two main components of the PrEP model framework: (1) the Bayesian network model of an adversary's perceived discovery risk, and (2) an aversion force-field component based on the physics of electrostatics, where discovery likelihood is the source for a repulsive electrostatic potential field. We have also introduced equations of motion for agents moving across a landscape towards an intended goal, while under the influence of geographically distributed aversive forces.

We have shown how coupling the Bayesian network and the aversion force component produces an aversion force field whose magnitude and direction plausibly represent the aversive influence that an adversary agent would feel when placed at some location in the discovery likelihood field.

We have also generated agent pathways through the aversion fields presented based on the agent equations of motion. The generated paths appear to be plausible in the context of the given aversion force field. We conclude that the formulation of the three elements combined thus far: Bayesian aversion likelihood model, aversion force field model, and agent equations of motion, suggest the approach at this stage is feasible. Planning for a more exacting demonstration is presently underway.